

Synthesis, Structure, Assembly, and Modulation of the CO₂ Adsorption Properties of a Zinc-Adeninate Macrocycle

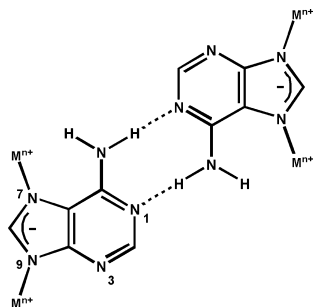
Jihyun An, Richard P. Fiorella, Steven J. Geib, and Nathaniel L. Rosi*

Department of Chemistry, University of Pittsburgh, 219 Parkman Avenue, Pittsburgh, Pennsylvania 15260

Received March 10, 2009; E-mail: nrosi@pitt.edu

Selective trapping of CO₂ from the emissions of coal-fired power plants is an important goal, which, if achieved in an economical fashion, could significantly contribute to the reduction of CO₂ emissions.¹ Herein, we present a porous material constructed from zinc-adeninate macrocycles that not only can be tailored to discriminate between gases of different kinetic diameter (e.g., CO₂ and N₂) but also can trap CO₂ within its cavities.

Our material design strategy relies on both the inherent recognition properties of biomolecules and their coordination chemistry. Biomolecules are intriguing material building blocks for a number of reasons: (1) they exist in biological systems and are thus likely biologically compatible; (2) they often have multiple metal coordination sites; and (3) they exhibit molecular recognition and self-assembling characteristics that could ultimately translate into interesting material properties.^{2–4} Metal ion coordination chemistry is potentially useful for directing the assembly of simple biomolecule building blocks into crystalline solid-state materials that exhibit accessible pores or channels within their structures.^{3,5} In this communication, we establish that adenine biomolecular building blocks can be used to construct zinc-adeninate macrocycles that self-assemble via multiple cooperative adenine–adenine hydrogen bonding interactions into porous structures. We also demonstrate that by tuning the activation temperature prior to gas adsorption studies, we can modulate the size of the pore aperture to allow for selective discrimination and sequestration of adsorbate gases.



Adenine, a purine nucleobase, is ideal for constructing porous biomolecular assemblies because (1) it is rigid, (2) it has multiple possible coordination sites, and (3) it offers the potential of assembly through both metal coordination and adenine–adenine hydrogen bonding interactions (*vide infra*).² Adeninate (deprotonation at N9) can coordinate metal ions through any of its five nitrogens. In fact, various complexes in which adenine is bound to metal ions principally through a combination of the N1, N3, N7, and N9 coordination sites have been isolated.⁶ However, exclusive coordination at the N7 and N9 sites is rare for crystalline materials.⁷ We reasoned that restricting the metal coordination to these sites would allow the amino group and N1 to participate in hydrogen bonding, thus affording an alternative mode for hierarchical assembly and another means for imparting structural rigidity. To

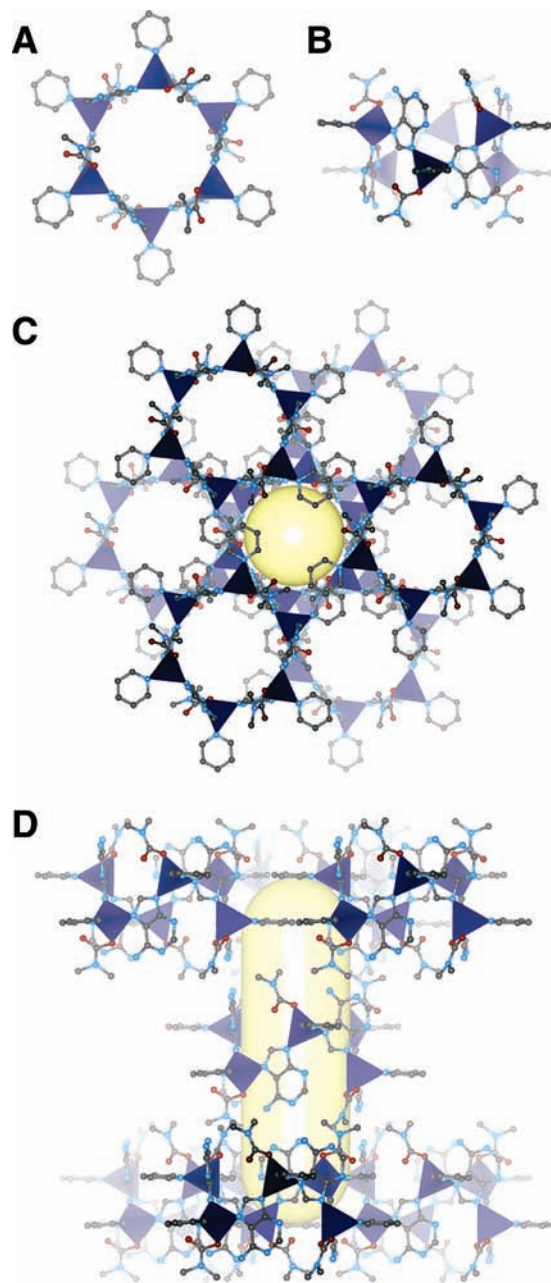


Figure 1. Top (A) and side (B) views of a single Zn₆(adeninate)₆-(pyridine)₆(dimethylcarbamate)₆ macrocycle (Zn²⁺, dark blue; C, dark gray; N, light blue; O, red; H omitted for clarity). The macrocycles pack into layers which are held together by hydrogen bonds between macrocycles in adjacent layers. The 3-D packing of the macrocycles within the crystal structure (C, D) results in the formation of large tubular cavities (yellow cylinder).

access structures that exploit this coordination motif, we performed a synthesis in which a mixture of adenine and zinc nitrate was dissolved in dimethylformamide (DMF) and pyridine. Pyridine was used as a base to facilitate adenine deprotonation at N9 and also to compete with N1 and N3 for coordination to Zn^{2+} . Heating this solution resulted in formation of a zinc-adeninate hexameric macrocycle, $\text{Zn}_6(\text{adeninate})_6(\text{pyridine})_6(\text{dimethylcarbamate})_6$. Single crystal X-ray diffraction data (Figure 1) revealed that six Zn^{2+} occupy the vertices of the macrocycle and adeninates bridge the Zn^{2+} through their imidazolate nitrogens. Each Zn^{2+} binds in a tetrahedral fashion to two adeninates, one pyridine molecule, and one dimethylcarbamate anion (formed in situ) (Figure 1A,B).⁸

Since only the imidazolate nitrogens of the adeninate coordinate the Zn^{2+} , N1 and the amino group remain available for hydrogen bonding. The macrocycles self-assemble into an extended structure via cooperative adeninate–adeninate hydrogen bonding interactions. This structure consists of alternating layers of macrocycles that stack in an a-b-c fashion. Each macrocycle forms a total of 12 hydrogen bonds (two per adeninate) with its six nearest-neighbor macrocycles within the structure. This packing motif results in the formation of cylindrical cavities ($\sim 5 \times 20 \text{ \AA}$) arranged periodically throughout the 3-D structure. The confines of each cavity are defined by one central macrocycle and fragments of the six nearest-neighbor macrocycles. Although free solvent molecules could not be resolved from the X-ray data, Platon analysis⁹ revealed significant residual electron density within the cavities, which we attribute to DMF guest molecules. Elemental analysis (EA) and thermal gravimetric analysis (TGA) data both suggest that ~ 10.5 DMF molecules per macrocycle reside within the structure.

Given that the assembled 3-D macrocycle structure exhibits large cavities, we were naturally interested in evaluating its porosity. Although many crystal structures of macrocyclic compounds exhibit 1-D channels in the solid state, few exhibit permanent porosity upon removal of guest molecules.¹⁰ This collapse is likely due to weak interactions between the neighboring macrocycles within the structure, which may lead to structural shear and obstruction of the channels upon guest removal. In our case, though, we reasoned that the strong adenine–adenine hydrogen bonding interactions between adjacent macrocycles might serve to lock the macrocycles in place and stabilize the crystal structure upon removal of guest molecules.

Inspection of the structure reveals that three pyridine rings occlude the entrance to each cavity, resulting in an aperture measuring only $\sim 1.2 \text{ \AA}$. To access the cavities, we needed to first remove a portion of the pyridine molecules to increase the pore aperture and allow diffusion of guest molecules within the structure. TGA studies were performed to assess the stability of the assembled structure and the mobility of the free DMF and coordinated pyridine molecules. We observed a 44% weight loss upon heating to $125 \text{ }^\circ\text{C}$, which corresponds roughly to the loss of the free DMF molecules and a fraction of the coordinated pyridines, based on EA data collected for the heated sample. Remarkably, the powder X-ray diffraction pattern of the heated sample matches that of the as-synthesized material (Figure 2A), indicating that the material maintains its structural integrity despite loss of DMF and coordinated pyridine, an aspect that points toward the utility of the multiple hydrogen bond interactions for generating a structurally robust material.

Encouraged by these results, we surmised that activating the material at $125 \text{ }^\circ\text{C}$ would effectively widen the cavity aperture (via loss of coordinated pyridine), allowing evacuation of guest molecules from the material. Indeed, sorption studies performed on the material after $125 \text{ }^\circ\text{C}$ activation revealed a small uptake of

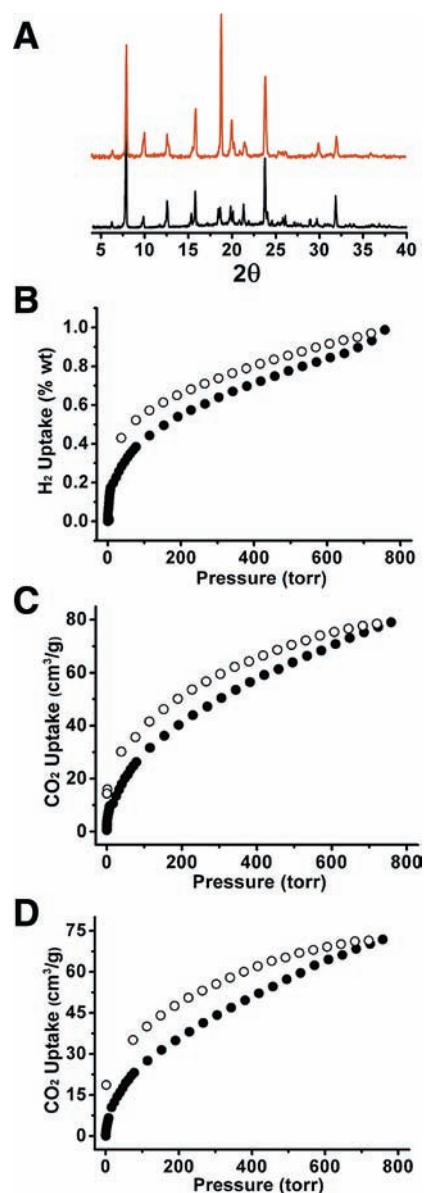


Figure 2. (A) Powder X-ray diffraction patterns for the as-synthesized material (black) and the material after heating to $125 \text{ }^\circ\text{C}$ (red). (B) Hydrogen sorption isotherm (77 K) for material activated at $125 \text{ }^\circ\text{C}$. Carbon dioxide sorption isotherms (273 K) for material activated at $125 \text{ }^\circ\text{C}$ (C) and $100 \text{ }^\circ\text{C}$ (D) ((●) adsorption; (○) desorption).

nitrogen (N_2 ; 77 K) (Supporting Information) and a comparatively large uptake of both hydrogen (H_2 ; 77 K) (Figure 2B) and carbon dioxide (CO_2 ; 273 K) (Figure 2C), which is likely due to the different kinetic diameters for the three gases (N_2 , 3.64 \AA ; CO_2 , 3.3 \AA ; H_2 , 2.89 \AA).¹¹ The maximum H_2 uptake is ~ 1 weight percent at 77 K and 1 atm which is similar to the uptake of many microporous metal–organic framework (MOF) materials.¹² Significantly, the H_2 isotherm was steep in the low pressure region, indicating a high affinity of the adsorbed H_2 to the material, which may be due to vacant coordination sites on the Zn^{2+} that result from removal of some of the coordinated pyridine molecules.¹²

Interestingly, the isotherms for both H_2 and CO_2 exhibited significant hysteresis upon desorption.¹³ We hypothesized this could be due to hindered diffusion through the narrow pore apertures.¹⁴ To understand the origin of the hysteresis, we compared the CO_2 sorption isotherm of the material activated at $125 \text{ }^\circ\text{C}$ (2) (Figure 2C) to the CO_2 isotherm of the material activated at $100 \text{ }^\circ\text{C}$ (3)

(Figure 2D). The hysteresis was more dramatic for **3**. Upon desorption, **2** retained ~38% of its sorbed CO₂ at 40 Torr while **3** retained nearly 45% of its sorbed CO₂ at the same desorption pressure. This observation suggests that the hysteresis is indeed likely due to a gating effect caused by the narrow pore apertures. Activation at 125 °C resulted in a greater loss of coordinated pyridine compared to activation at 100 °C; therefore, we expect that the pore aperture for **3** is smaller than that for **2**, consequently resulting in a more dramatic hysteresis. The decrease in the pore aperture is supported by N₂ sorption experiments: like typical microporous materials, **2** exhibits some N₂ uptake at low pressures, although it does not reach saturation, whereas **3** does not readily adsorb N₂ (Supporting Information). Collectively, these sorption data suggest that the size of the pore aperture can be tailored to tune the material's ability to selectively trap CO₂ within its structure.

It is important to note that small sorbent-induced structural rearrangements¹⁵ may also contribute to the hysteresis. However, if this were the case, we would expect to see more dramatic hysteresis for **2** rather than **3**, because more structural components have been removed for **2**. We also considered that strong sorbate open-metal site interactions might contribute to the observed hysteresis. However, using the Dubinin–Radushkevich (DR) equation, the isosteric heat of adsorption was calculated to be ~21 kJ/mol at 273 K. This value is much smaller than those usually observed for chemisorption¹⁶ and also smaller than those observed for MOF materials with open-metal sites.¹⁷ Therefore, we reason that sorbate open-metal site interactions do not contribute significantly to the hysteresis.

To conclude, we have demonstrated that strong biomolecular hydrogen bonding interactions can be used to assemble zinc adeninate macrocycles into robust materials that exhibit large cavities within their structures. Careful removal of the coordinated pyridine molecules that “gate” the cavity entrances allows for modulation of the cavity aperture dimensions and therefore discrimination of adsorbate molecules based on their kinetic diameter. In addition, by tuning the aperture size, we can adjust the amount of CO₂ that can be trapped within the structure. Together, these results point toward the potential utility of this material in gas separation and sequestration applications.¹⁸ We note that the specific strategy we present for modulating pore aperture dimensions to impart specific gas sorption properties is unique. We believe that this strategy can be extended to the design of new porous materials that have controllable pore “gates” that can be opened or closed to affect the capture and release of specific gas molecules.

Acknowledgment. Funding for this work was provided by the University of Pittsburgh and the American Chemical Society Petroleum Research Fund (PRF 47601-G10). The authors thank the Department of Mechanical Engineering and Materials Science as well as the Petersen Institute for Nanoscience and Engineering (PINSE) for access to XRPD instrumentation. The authors also thank Prof. Tara Meyer for providing thoughtful input on the manuscript.

Supporting Information Available: Experimental procedures, crystallographic data, and additional supporting data. This material is available free of charge via the Internet at <http://pubs.acs.org>.

References

- (1) Kintisch, E. *Science* **2007**, *317*, 184–186.
- (2) Sivakova, S.; Rowan, S. J. *Chem. Soc. Rev.* **2005**, *34*, 9–21.
- (3) Bodwin, J. J.; Cutland, A. D.; Malkani, R. G.; Pecoraro, V. L. *Coord. Chem. Rev.* **2001**, *216–217*, 489–512.
- (4) Sessler, J. L.; Lawrence, C. M.; Jayawickramarajah, J. *Chem. Soc. Rev.* **2007**, *36*, 314–325.
- (5) (a) Eddaoudi, M.; Moler, D. B.; Li, H. L.; Chen, B. L.; Reineke, T. M.; O’Keeffe, M.; Yaghi, O. M. *Acc. Chem. Res.* **2001**, *34*, 319–330. (b) Kitagawa, S.; Kitaura, R.; Noro, S. *Angew. Chem., Int. Ed.* **2004**, *43*, 2334–2375. (c) Ferey, G. *Chem. Soc. Rev.* **2008**, *37*, 191–214. (d) Vaidyanathan, R.; Bradshaw, D.; Rebilly, J. N.; Barrio, J. P.; Gould, J. A.; Berry, N. G.; Rosseinsky, M. J. *Angew. Chem., Int. Ed.* **2006**, *45*, 6495–6499. (e) Suzuki, K.; Kawano, M.; Sato, S.; Fujita, M. *J. Am. Chem. Soc.* **2007**, *129*, 10652–10663. (f) Rauterkus, M. J.; Krebs, B. *Angew. Chem., Int. Ed.* **2004**, *43*, 1300–1303. (g) Armentano, D.; Mastropietro, T. F.; Julve, M.; Rossi, R.; Rossi, P.; De Munno, G. *J. Am. Chem. Soc.* **2007**, *129*, 2740–2741. (h) Lee, H. Y.; Kampf, J. W.; Park, K. S.; Marsh, E. N. G. *Cryst. Growth Des.* **2008**, *8*, 296–303. (i) Salgado, E. N.; Lewis, R. A.; Faraone-Mennella, J.; Tezcan, F. A. *J. Am. Chem. Soc.* **2008**, *130*, 6082–6083.
- (6) (a) Navarro, J. A. R.; Lippert, B. *Coord. Chem. Rev.* **1999**, *185–186*, 653–667. (b) Garcia-Teran, J. P.; Castillo, O.; Luque, A.; Garcia-Couceiro, U.; Roman, P.; Lezama, L. *Inorg. Chem.* **2004**, *43*, 4549–4551. (c) Gonzalez-Perez, J. M.; Alarcon-Payer, C.; Castineiras, A.; Pivetta, T.; Lezama, L.; Choquesillo-Lazarte, D.; Crisponi, G.; Niclos-Gutierrez, J. *Inorg. Chem.* **2006**, *45*, 877–882. (d) Purohit, C. S.; Verma, S. *J. Am. Chem. Soc.* **2006**, *128*, 400–401. (e) Yang, E. C.; Zhao, H. K.; Ding, B.; Wang, X. G.; Zhao, X. J. *New J. Chem.* **2007**, *31*, 1887–1890. (f) Marzotto, A.; Ciccarese, A.; Clemente, D. A.; Valle, G. *J. Chem. Soc., Dalton Trans.* **1995**, 1461–1468. (g) Suzuki, T.; Hirai, Y.; Monjushiro, H.; Kaizaki, S. *Inorg. Chem.* **2004**, *43*, 6435–6444.
- (7) (a) Prizant, L.; Olivier, M. J.; Rivest, R.; Beauchamp, A. L. *J. Am. Chem. Soc.* **1979**, *101*, 2765–2767. (b) Korn, S.; Sheldrick, W. S. *Inorg. Chim. Acta* **1997**, *254*, 85–91. (c) Rojas-Gonzalez, P. X.; Castineiras, A.; Gonzalez-Perez, J. M.; Choquesillo-Lazarte, D.; Niclos-Gutierrez, J. *Inorg. Chem.* **2002**, *41*, 6190–6192.
- (8) Dell’Amico, D. B.; Calderazzo, F.; Labella, L.; Marchetti, F. *Inorg. Chim. Acta* **2003**, *350*, 661–664.
- (9) van der Sluis, P.; Spek, A. L. *Acta Crystallogr., Sect. A* **1990**, *46*, 194–201.
- (10) (a) Dewal, M. B.; Lufaso, M. W.; Hughes, A. D.; Samuel, S. A.; Pellechia, P.; Shimizu, L. S. *Chem. Mater.* **2006**, *18*, 4855–4864. (b) Lim, S.; Kim, H.; Selvapalam, N.; Kim, K. J.; Cho, S. J.; Seo, G.; Kim, K. *Angew. Chem., Int. Ed.* **2008**, *47*, 3352–3355. (c) Dobrzanska, L.; Lloyd, G. O.; Raubenheimer, H. G.; Barbour, L. J. *J. Am. Chem. Soc.* **2005**, *127*, 13134–13135. (d) Chatterjee, B.; Noveron, J. C.; Resendiz, M. J. E.; Liu, J.; Yamamoto, T.; Parker, D.; Cinke, M.; Nguyen, C. V.; Arif, A. M.; Stang, P. J. *J. Am. Chem. Soc.* **2004**, *126*, 10645–10656.
- (11) (a) Breck, D. W. *Zeolite Molecular Sieves*; John Wiley & Sons: New York, 1974; p 636. (b) N₂ adsorption isotherms for **2** collected at 273 K also revealed nonporous behavior.
- (12) (a) Rowsell, J. L. C.; Yaghi, O. M. *Angew. Chem., Int. Ed.* **2005**, *44*, 4670–4679. (b) Dinca, M.; Long, J. R. *Angew. Chem., Int. Ed.* **2008**, *47*, 6766–6779.
- (13) (a) Zhao, X. B.; Xiao, B.; Fletcher, A. J.; Thomas, K. M.; Bradshaw, D.; Rosseinsky, M. J. *Science* **2004**, *306*, 1012–1015. (b) Choi, H. J.; Dinca, M.; Long, J. R. *J. Am. Chem. Soc.* **2008**, *130*, 7848–7850.
- (14) (a) Gregg, S. J.; Sing, K. S. W. *Adsorption, Surface Area, and Porosity*; Academic Press: New York, 1967; p 145. (b) Pan, L.; Adams, K. M.; Hernandez, H. E.; Wang, X. T.; Zheng, C.; Hattori, Y.; Kaneko, K. *J. Am. Chem. Soc.* **2003**, *125*, 3062–3067.
- (15) Cussen, E. J.; Claridge, J. B.; Rosseinsky, M. J.; Kepert, C. J. *J. Am. Chem. Soc.* **2002**, *124*, 9574–9581.
- (16) Hayward, D. O.; Trapnell, B. M. W. *Chemisorption*, 2nd ed.; Butterworths: London, 1964.
- (17) Caskey, S. R.; Wong-Foy, A. G.; Matzger, A. J. *J. Am. Chem. Soc.* **2008**, *130*, 10870–10871.
- (18) (a) Chen, B. L.; Ma, S. Q.; Hurtado, E. J.; Lobkovsky, E. B.; Zhou, H. C. *Inorg. Chem.* **2007**, *46*, 8490–8492. (b) Ma, S. Q.; Sun, D. F.; Wang, X. S.; Zhou, H. C. *Angew. Chem., Int. Ed.* **2007**, *46*, 2458–2462. (c) Banerjee, R.; Phan, A.; Wang, B.; Knobler, C.; Furukawa, H.; O’Keeffe, M.; Yaghi, O. M. *Science* **2008**, *319*, 939–943.

JA901869M